Multi-dimensional Evaluation Methods for Enhancing the Teaching Effectiveness of Mechanical Courses

Lin Chang[a*], Fangxiang Zhuang[b], Jiehua Gao[c], Jiamiao Wei[d], Chenxin Xie[e]

College of Engineering, Huzhou University, Huzhou, China

[a*]Corresponding author: 18905370986@163.com
[b]19857297521@163.com, [c]17862686792@163.com
[d]w20031628@163.com, [e]13738803935@163.com

Abstract. Processing error is a key factor affecting the accuracy and quality of machined components. However, in the current course of Mechanical Drawing, the teaching of processing error and surface roughness is relatively weak, which means students cannot combine practical problems with theoretical knowledge. To solve this problem, novel multi-dimensional processing error assessment methods based on spectral analysis are introduced. This method not only overcomes the limitations of the traditional surface roughness evaluation but also reveals more in-depth and extensive error distribution characteristics and information. Introducing this method into teaching will provide more effective analytical tools for the teaching field of mechanical specialties, thus deepening students' understanding and application of advanced analytical techniques.

Keywords: Mechanical drawing; Machining errors; Evaluation parameters; Roughness; Fourier transforms

1 Introduction

Traditionally, teaching machining accuracy has focused on component geometry and limited machined features in "Mechanical Drawing" [1-2]. However, evolving analytical techniques, like the Fourier transforms, can enhance course content, expanding knowledge and improving data interpretation [3-4]. Applying these mathematical tools allows students to understand surface error causes and optimize machining processes. Keeping teaching methods updated with technology is crucial. This paper discusses using multi-dimensional error assessment in mechanical courses to boost teaching outcomes and equip students with skills to address machining errors effectively.

2 Conventional Assessing Methods

Surface roughness is important in evaluating mechanical quality in "Mechanical Drawing", impacting wear resistance, fatigue strength, and product sealing. Traditional teaching methods often cover only the basics of roughness, lacking detailed analysis of

Y. Kuang et al. (eds.), *Proceedings of the 2024 5th International Conference on Education, Knowledge and Information Management (ICEKIM 2024)*, Atlantis Highlights in Computer Sciences 22,
https://doi.org/10.2991/978-94-6463-502-7_88

its significance and control in design and manufacturing. This can hinder students' understanding and optimization skills. Typically, as shown in Fig. 1, two main roughness evaluation parameters are taught, but without a deeper exploration of their practical implications [5].

i. R_a is defined as the arithmetic mean of the absolute values of the longitudinal coordinate $Z(x_L)$ over the sampling length l_r (the selected line is denoted as x_L).

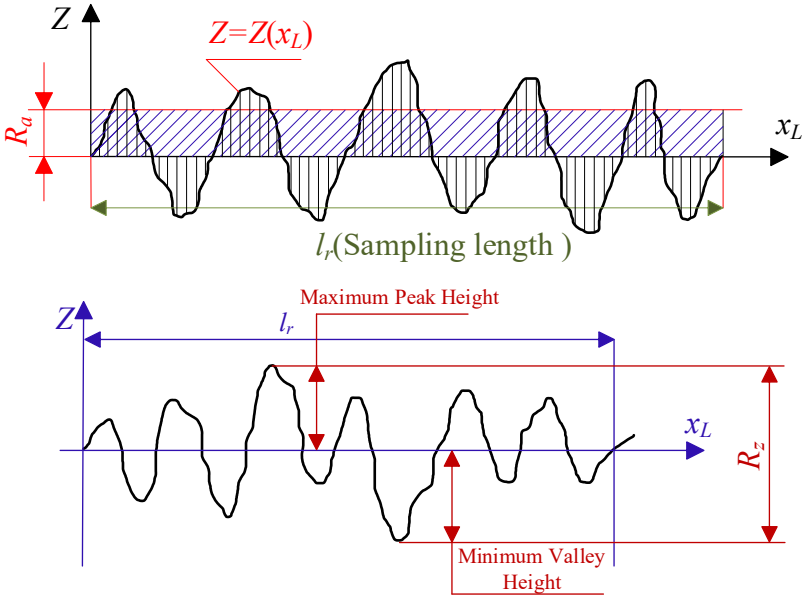

Fig. 1. Schematic diagram of the solution process of R_a and R_Z

$$R_a = \frac{1}{l_r}\int_0^{l_r}|Z(x)|\mathrm{d}x \tag{1}$$

ii. R_Z is defined as the height difference between the maximum peak height and the maximum valley depth in a sampling length.

To overcome the deficiencies of the existing teaching methods, we introduce a multi-dimensional processing error assessment method. Only focuses on the size of the processing error, but also concerns analysis such as the distribution characteristics and periodic variation of the errors, through which, the assessment results can be effectively traced back to the error sources. Then, we can more comprehensively understand the characteristics and patterns of processing errors, and provide more targeted guidance for error control and optimization. At the same time, the multi-dimensional machining error assessment method can also be combined with the surface roughness evaluation to assess the quality and performance of mechanical parts from multiple perspectives, and ultimately improve students' understanding and mastery of this issue.

3 Multi-dimensional Assessment Methods

The Fourier Transform transforms a signal from time to frequency domain, exposing its frequency components. It's used in spatial analysis to find periodic features in images and in sequence analysis to detect fluctuations in data series. This is useful for data compression, filtering, and feature extraction, making it ideal for analyzing processing errors. We begin with the sequence Fourier transform. First, the process of spatial Fourier transform is given as shown in Equation (2) [6]:

$$F(u,v) = \sum_{x=0}^{M-1} \sum_{y=0}^{N-1} f(x,y) \mathrm{e}^{-\mathrm{j}2\pi\left(\frac{ux}{M}+\frac{vy}{N}\right)} \tag{2}$$

In Equation (2), f(x, y) represents a matrix of size $M \times N$, $x = 0, 1, 2, \ldots, M\text{-}1$ and $y = 0, 1, 2, \ldots, N\text{-}1$, j is an imaginary unit, and $F(u, v)$ denotes the Fourier transform of $f(x, y)$. A two-dimensional spectrum map can be obtained by performing a spatial domain Fourier transform on the surface shape of a selected area through Equation (2), which can extract the frequency magnitude distributions.

The sequence Fourier transform computes for a one-dimensional sequence as an object. If the height of the component on one of the lines is chosen as the analysis object ($x(n)$, n=1, 2, 3, ..., N, N is the total number), its height characteristics can also be given using the Fourier transform of the sequence:

$$x(n) = \mathrm{e}^{\mathrm{j}(2\pi\beta n/N+\theta)} \tag{3}$$

where β is the frequency multiplier and θ is the initial phase (which often reflects height information). Further, the Fourier transform X of $x(n)$ can be expressed as [7]:

$$X(k) = \frac{1}{N} \sum_{n=0}^{N-1} \mathrm{e}^{\mathrm{j}\theta} \mathrm{e}^{\mathrm{j}2\pi n\beta/N} \mathrm{e}^{-\mathrm{j}2\pi kn/N} = \frac{1}{N} \mathrm{e}^{\mathrm{j}\theta} \sum_{n=0}^{N-1} \mathrm{e}^{\mathrm{j}2\pi(\beta-k)n/N} \tag{4}$$

where k is a frequency domain variable (sequence type). Further, it can be obtained:

$$X(k) = \frac{1}{N} \cdot \frac{\sin[\pi(\beta-k)]}{\sin\left[\frac{\pi(\beta-k)}{N}\right]} \cdot \mathrm{e}^{\mathrm{j}\left[\theta+\frac{N-1}{N}(\beta-k)\pi\right]} \tag{5}$$

The window function is introduced to minimize the effect of the undesirable distribution of the edges, then for a complex signal $\{x(n) = \mathrm{e}^{\mathrm{j}\omega^* n}, n \in [0, N-1]\}$ (ω^* is the corner frequency), its form with an additive window F_g can be given by the following equation [8]:

$$X(k) = F_\mathrm{g}(k\Delta\omega - \omega^*) \mathrm{e}^{-\mathrm{j}\tau(k\Delta\omega-\omega^*)} \tag{6}$$

where $\Delta\omega$ is the frequency resolution and τ is the group delay. For a complex signal considering a non-zero initial phase, its add-windowed series Fourier transform can be given by the following equation (A is the signal amplitude and n_0 is the sequence delay) [9]:

$$X(k) = A\mathrm{e}^{\mathrm{j}(\theta-\omega^* n_0)} \cdot F_\mathrm{g}(k\Delta\omega - \omega^*) \mathrm{e}^{-\mathrm{j}\tau(k\Delta\omega-\omega^*)} \tag{7}$$

Hereafter, the height of the surface shape of the component is normalized to between 0 and 1 for the convenience of the display. Taking the surface height as an example (displayed as shown in Fig. 2), its distribution can be given by the spatial Fourier transform and the serial Fourier transform, as shown follows.

Performing a spatial Fourier transform on the above surface shape and extracting the frequency amplitudes, the result shown in Fig. 3 is obtained. Further, using the sequence Fourier transform, the heights are extracted from the 250th horizontal (row) and 250th vertical (columns) directions, respectively, as shown in Fig. 3.

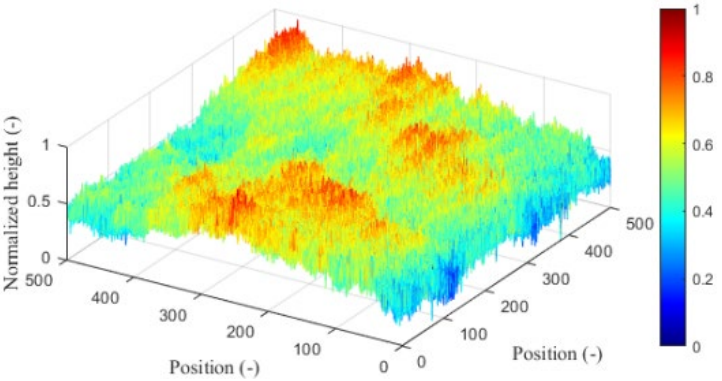

Fig. 2. Height distribution of surface shapes of a component

Measurement methods might not accurately capture surface features at edges, hence sequence windowing, like the Blackman window used here [10], is an effective solution. Further, from the spectral characteristics shown in Figs. 2 ~ 3, the low-frequency machining error that can determine the basic distribution of the surface shape is dominant, but the high-frequency error that influences the roughness and smoothness still exists and is accompanied by a certain fluctuation amplitude. This means that reverse error tracing and error control are necessary.

Typically, the machining errors at each frequency band correspond to the corresponding machining steps. The results of the quantitative analysis of the machining errors can in turn help to optimize the process. This also usually means a balance between economy and precision. For example, in the machining of optical components, surface machining errors directly affect the performance of the part, which in turn has a non-negligible impact on the imaging and output performance of the optical system.

The instrumentation used for measurement and the processing of the detected signals are also very important. In machining, individualized machining and inspection requirements determine the measurement methods used. Contact measurements are usually easy to realize, but are relatively inefficient. Non-contact measurement methods (represented by interferometry), on the other hand, have a high measuring accuracy, but the equipment is expensive and the processing methods are complex.

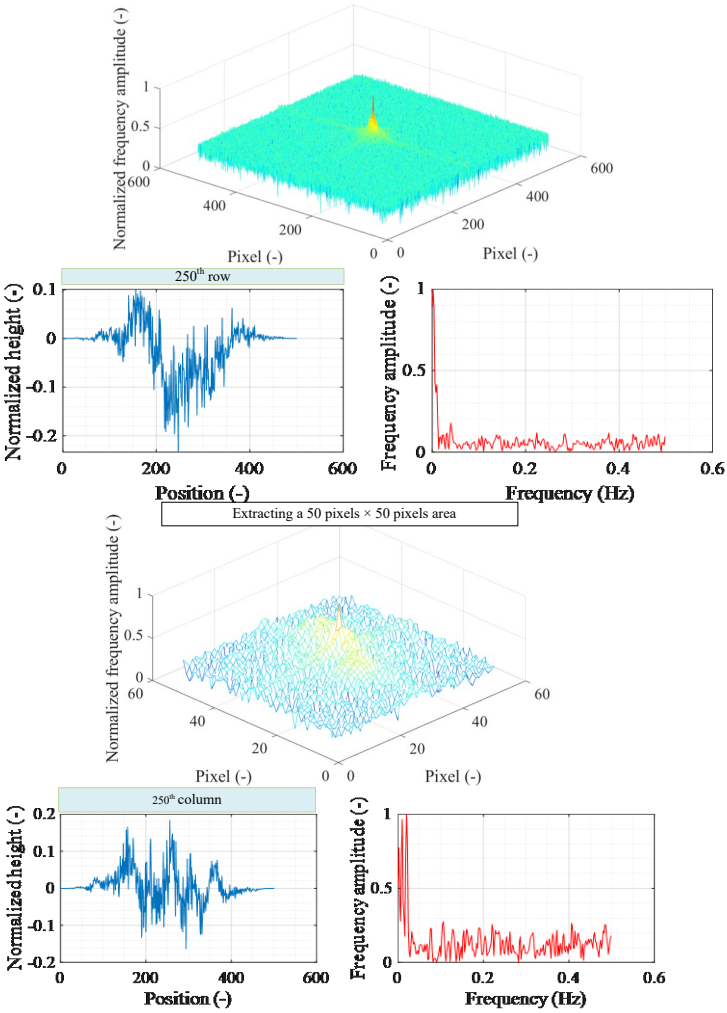

Fig. 3. Spatial Fourier Transform results

The two spectral analysis methods provide the possibility of multi-dimensional interpretation of machining errors and provide a basis for the control of these errors, which can be expected to be an effective quantitative analysis technique in industrial machining.

4 Conclusion

Traditionally, Mechanical Drawing education has focused on component dimensions and basic machining features (R_a and R_Z), but advancements allow for the introduction of advanced quantified methods like spatial and sequence Fourier transforms.

These enrich students' understanding by enabling the analysis of frequency distribution characteristics, which are crucial for identifying machining errors. Fourier transform techniques also offer insights into surface roughness spectral characteristics, aiding in machining process optimization. Incorporating these modern analysis techniques not only boosts students' expertise but also ignites their curiosity and enthusiasm for exploring contemporary manufacturing technologies.

Acknowledgment

The research is sponsored by the Education and Teaching Project (JG202254) of Huzhou University.

References

1. Xu Y, Zhang C, Xu Z, Kong C, Tang D, Deng X, et al. Tolerance Information Extraction for Mechanical Engineering Drawings – A Digital Image Processing and Deep Learning-based Model. CIRP J Manuf Sci Technol 2024;50:55–64. https://doi.org/10.1016/j.cirpj.2024.01.013.
2. Pan Z, Yu Y, Xiao F, Zhang J. Recovering building information model from 2D drawings for mechanical, electrical and plumbing systems of ageing buildings. Autom Constr 2023;152:104914. https://doi.org/10.1016/j.autcon.2023.104914.
3. Servin M, Estrada JC, Quiroga JA, Mosino JF, Cywiak M. Noise in phase shifting interferometry. Opt Express 2009;17:8789. https://doi.org/10.1364/oe.17.008789.
4. Chang L, Yu Y. Wavelength-tuning phase-shifting interferometry of transparent plates using sub-signal frequency correction. Measurement 2022;205:112157. https://doi.org/10.1016/j.measurement.2022.112157.
5. Pilgar CM, Fernandez AM, Segurado J. A fatigue life model accounting for the combined effect of surface roughness and microstructure : Application to SLM fabricated Hastelloy-X. Int J Fatigue 2024;184:108298. https://doi.org/10.1016/j.ijfatigue.2024.108298.
6. Nakayama S, Toba H, Fujiwara N, Gemma T, Takeda M. En-hanced Fourier-transform method for high-density fringe analysis by iterative spectrum narrowing. Appl Opt 2020;59:9159. https://doi.org/10.1364/ao.402415.
7. Jin T, Chen Y, Flesch RCC. A novel power harmonic analysis method based on Nuttall-Kaiser combination window double spectrum interpolated FFT algorithm. J Electr Eng 2017;68:435–43. https://doi.org/10.1515/jee-2017-0078.
8. Ochoa NA, Silva-Moreno AA. Normalization and noise-reduction algorithm for fringe patterns. Opt Commun 2007;270:161–8. https://doi.org/10.1016/j.optcom.2006.09.062.
9. Yan Chen, Xiaohu Wang, Xiong Liu, Zhiquan Ye TW. Aerody-namic damping analysis of horizontal axis wind turbine blade in steady stall. Acta Energiae Solaris Sin 2011;32:1294–302. https://doi.org/10.1051/forest.
10. Chang L, Valyukh S, He T, Yu Y. Multisurface Interferometric Algorithm and Error Analysis with Adaptive Phase Shift Matching. IEEE Trans Instrum Meas 2022;71. https://doi.org/10.1109/TIM.2021.3137160.